Compensation of the Transmitter I/Q Skew, Gain, and Phase Imbalance in Subcarrier Multiplexing Receivers

Mario R. Hueda and José L. Correa Lust

September 2017

Abstract

An 8×8 adaptive equalizer has been proposed recently in [1] to compensate the effectsof transmitter I/Q skew in subcarrier multiplexing (SCM) schemes. This report investigates in more detail the performance and complexity of the compensator for the transmitter I/Q skew and quadrature error in SCM systems. Based on this study, we derive a reduced complexity 8×8 adaptive equalizer for compensating transmitter I/Q imbalance and skew. Compared to the previous solution [1], we find that the complexity of the 8×8 adaptive equalizer can be reduced ~ 4 times without any impact on the receiver performance. Furthermore, and unlike to that reported in [2], we demonstrate that the phase and gain imbalance of the modulator (Tx) cannot be completely compensated at the receiver without amplifying the channel noise.

I. Impact of I/Q Skew on the SCM Signal

Let $s_1(t)$ and $s_2(t)$ be the baseband signal for subcarrier 1 and 2, respectively, given by

$$s_1(t) = \sum_k \left(a_{k,1}\mathbf{x} + b_{k,1}\mathbf{y}\right) g(t - kT), \tag{1}$$

$$s_2(t) = \sum_k \left(a_{k,2}\mathbf{x} + b_{k,2}\mathbf{y}\right) g(t - kT), \tag{2}$$

where $a_{k,i}$ and $b_{k,i}$ are the complex symbols for both polarizations of carrier i with $i \in \{1, 2\}$, $g(t)$ is the impulse response of the transmit filter, while $\mathbf{x}$ and $\mathbf{y}$ are vectors for both polarizations. Note that T is the symbol period at each subcarrier.

The transmit SCM signal can be written as

$$s(t) = s_1(t)e^{j\omega_c t} + s_2(t)e^{-j\omega_c t}, \tag{3}$$

where $\pm\omega_c$ are the angular frequencies of the subcarriers.

Consider that an I/Q skew is added before optical modulator. Then, it is possible to show that the resulting signal is

$$y(t) = s(t) \otimes b(t) + s^*(t) \otimes \overline{b}(t), \tag{4}$$

where $\otimes$ denotes convolution, while

$$b(t) = \frac{1}{2}\left[\delta(t+\tau/2) + \delta(t-\tau/2)\right], \tag{5}$$

$$\overline{b}(t) = \frac{1}{2}\left[\delta(t+\tau/2) - \delta(t-\tau/2)\right], \tag{6}$$

with τ being the I/Q skew introduced at the transmitter.

Then, the modulator introduces quadrature error resulting [3]

$$r(t) = \alpha y(t) + \beta y^*(t), \tag{7}$$

where

$$\alpha = \frac{1}{2}\left[(1-\epsilon)e^{j\phi/2} + (1+\epsilon)e^{-j\phi/2}\right], \tag{8}$$

$$\beta = \frac{1}{2}\left[(1-\epsilon)e^{-j\phi/2} - (1+\epsilon)e^{j\phi/2}\right], \tag{9}$$

with ϕ and ϵ being the phase and amplitude imbalance, respectively (note that both parameters are real numbers). Operating, we get

$$r(t) = s(t) \otimes f(t) + s^*(t) \otimes \overline{f}(t), \tag{10}$$

where

$$f(t) = \alpha b(t) + \beta\overline{b}(t) = \frac{(\alpha+\beta)}{2}\delta(t+\tau/2) + \frac{(\alpha-\beta)}{2}\delta(t-\tau/2) \tag{11}$$

$$\overline{f}(t) = \alpha\overline{b}(t) + \beta b(t) = \frac{(\alpha+\beta)}{2}\delta(t+\tau/2) - \frac{(\alpha-\beta)}{2}\delta(t-\tau/2). \tag{12}$$

The first term in (10) can be expressed as

$$\begin{aligned} s(t) \otimes f(t) &= s_1(t)e^{j\omega_c t} \otimes f(t) + s_2(t)e^{-j\omega_c t} \otimes f(t) \qquad (13)\\ &= e^{j\omega_c t}\sum_k \left(a_{k,1}\mathbf{x} + b_{k,1}\mathbf{y}\right) h_{e,1}(t-kT) + e^{-j\omega_c t}\sum_k \left(a_{k,2}\mathbf{x} + b_{k,2}\mathbf{y}\right) h_{e,2}(t-kT) \end{aligned}$$

where $h_{e,1}(t)$ and $h_{e,2}(t)$ are the baseband equivalent channel responses given by

$$h_{e,1}(t) = g(t) \otimes f(t)e^{-j\omega_c t}, \tag{14}$$

$$h_{e,2}(t) = g(t) \otimes f(t)e^{j\omega_c t}. \tag{15}$$

Similarly, the second term in (10) results in

$$\begin{aligned} s^*(t) \otimes \overline{f}(t) &= s_1^*(t)e^{-j\omega_c t} \otimes \overline{f}(t) + s_2^*(t)e^{j\omega_c t} \otimes \overline{f}(t) \qquad (16)\\ &= e^{-j\omega_c t} \sum_k \left(a_{k,1}^*\mathbf{x} + b_{k,1}^*\mathbf{y}\right) \overline{h}_{e,1}(t-kT) + e^{j\omega_c t} \sum_k \left(a_{k,2}^*\mathbf{x} + b_{k,2}^*\mathbf{y}\right) \overline{h}_{e,2}(t-kT) \end{aligned}$$

where

$$\overline{h}_{e,1}(t) = g(t) \otimes \overline{f}(t)e^{j\omega_c t}, \tag{17}$$

$$\overline{h}_{e,2}(t) = g(t) \otimes \overline{f}(t)e^{-j\omega_c t}. \tag{18}$$

The received signal $r(t)$ given by (10) is demodulated by two carriers $e^{\pm j\omega_c t}$ and filtered by a lowpass filter to get two baseband signals, $r_1(t)$ and $r_2(t)$. From (13) and (16) we can obtain

$$r_1(t) = \sum_k \left(a_{k,1}\mathbf{x} + b_{k,1}\mathbf{y}\right) h_{e,1}(t-kT) + \sum_k \left(a_{k,2}^*\mathbf{x} + b_{k,2}^*\mathbf{y}\right) \overline{h}_{e,2}(t-kT) \tag{19}$$

$$r_2(t) = \sum_k \left(a_{k,2}\mathbf{x} + b_{k,2}\mathbf{y}\right) h_{e,2}(t-kT) + \sum_k \left(a_{k,1}^*\mathbf{x} + b_{k,1}^*\mathbf{y}\right) \overline{h}_{e,1}(t-kT) \tag{20}$$

Operating,

$$\begin{aligned} r_1(t) &= \mathbf{x}\sum_k a_{k,1}h_{e,1}(t-kT) + a_{k,2}^*\overline{h}_{e,2}(t-kT) + \mathbf{y}\sum_k b_{k,1}h_{e,1}(t-kT) + b_{k,2}^*\overline{h}_{e,2}(t-kT)\\ &= r_{1,x}(t)\mathbf{x} + r_{1,y}(t)\mathbf{y} \qquad (21)\\ r_2(t) &= \mathbf{x}\sum_k a_{k,2}h_{e,2}(t-kT) + a_{k,1}^*\overline{h}_{e,1}(t-kT) + \mathbf{y}\sum_k b_{k,2}h_{e,2}(t-kT) + b_{k,1}^*\overline{h}_{e,1}(t-kT)\\ &= r_{2,x}(t)\mathbf{x} + r_{2,y}(t)\mathbf{y} \qquad (22) \end{aligned}$$

where

$$r_{1,x}(t) = \sum_k a_{k,1} h_{e,1}(t - kT) + a^*_{k,2} \overline{h}_{e,2}(t - kT) \tag{23}$$

$$r_{1,y}(t) = \sum_k b_{k,1} h_{e,1}(t - kT) + b^*_{k,2} \overline{h}_{e,2}(t - kT) \tag{24}$$

$$r_{2,x}(t) = \sum_k a_{k,2} h_{e,2}(t - kT) + a^*_{k,1} \overline{h}_{e,1}(t - kT) \tag{25}$$

$$r_{2,y}(t) = \sum_k b_{k,2} h_{e,2}(t - kT) + b^*_{k,1} \overline{h}_{e,1}(t - kT) \tag{26}$$

We highlight the following facts:

- The transmit I/Q skew does not *combine* the polarizations, therefore ***each output of the 8x8 MIMO equalizer does not depend of all the inputs, i.e., to compensate the Tx mismatches, one polarization of Carrier 1 (e.g.,*** $r_{1,x}(t)$***) just needs information from one polarization of the Carrier 2 (e.g.,*** $r_{2,x}(t)$***)***.
- Unlike single carrier, ***the quadrature error caused by the Tx modulator does not introduce correlation between I/Q of a given polarization (e.g., note that*** $r_{1,x}(t)$ ***is independent on*** $a^*_{k,1}$***; it only depends on*** $a_{k,1}$***); its effect in SCM receivers is similar to the one caused by a I/Q skew***.

II. Analysis

A. Case 1: Impact of Quadrature Error ($\tau = 0$)

In the absence of I/Q skew (i.e., $\tau = 0$), we get

$$f(t) = \alpha\delta(t)$$

$$\overline{f}(t) = \beta\delta(t).$$

Since $f(t)e^{\pm j\omega_c t} = \alpha\delta(t)e^{\pm j\omega_c t} = \alpha\delta(t)$ and $\overline{f}(t)e^{\pm j\omega_c t} = \beta\delta(t)e^{\pm j\omega_c t} = \beta\delta(t)$, we get

$$h_{e,1}(t) = h_{e,2}(t) = \alpha g(t),$$

$$\overline{h}_{e,1}(t) = \overline{h}_{e,2}(t) = \beta g(t).$$

Figure 1 shows the responses for $\tau = 0T$, $\epsilon = 0.2$, and $\phi = 20^o$ obtained from simulations. We confirm the results predicted from the theory.

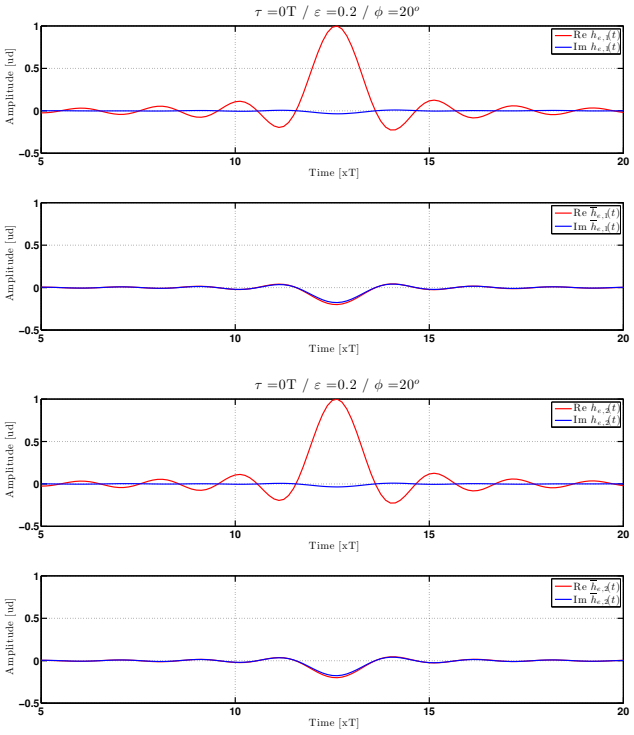

Figure 1. Example of the channel responses for $\tau = 0T$, $\epsilon = 0.2$, and $\phi = 20^o$

Next we evaluate the impact and compensation of the quadrature error on the receiver. Assuming that $g(t)$ is an ISI-free pulse, we can verify that the baud rate samples of the signals for a same polarization of both subcarriers result, e.g.,

$$r_{1,x}(n) = \alpha a_{n,1} + \beta a_{n,2}^* \tag{27}$$

$$r_{2,x}(n) = \alpha a_{n,2} + \beta a_{n,1}^* \tag{28}$$

Notice that we can detect $a_{n,1}$ and $a_{n,2}^*$ (instead of $a_{n,2}$) by considering the equivalent system

$$r_{1,x}(n) = \alpha a_{n,1} + \beta a_{n,2}^* \tag{29}$$

$$r_{2,x}^*(n) = \alpha^* a_{n,2}^* + \beta^* a_{n,1} \tag{30}$$

Thus, the baud-rate samples can be rewritten as

$$\begin{bmatrix} r_{1,x}(n) \\ r_{2,x}^*(n) \end{bmatrix} = \mathbf{M}_{\phi,\epsilon} \begin{bmatrix} a_{1,n} \\ a_{2,n}^* \end{bmatrix} \tag{31}$$

where

$$\mathbf{M}_{\phi,\epsilon} = \begin{bmatrix} \alpha & \beta \\ \beta^* & \alpha^* \end{bmatrix}. \tag{32}$$

To compensate the quadrature error at the receiver in order to obtain $a_{1,n}$ and $a_{2,n}^*$ (i.e., $a_{2,n}$), we use a linear transformation based on the matrix

$$\mathbf{M}_{\phi,\epsilon}{}^{-1} = \frac{1}{\det(\mathbf{M}_{\phi,\epsilon})} Adj(\mathbf{M}_{\phi,\epsilon}) = \frac{1}{|\alpha|^2 - |\beta|^2} \begin{bmatrix} \alpha^* & -\beta \\ -\beta^* & \alpha \end{bmatrix}. \tag{33}$$

Then, the power of the noise added *after* the Tx modulator will be amplified by a factor[1]

$$\begin{aligned} F &= \frac{|\alpha|^2 + |\beta|^2}{(|\alpha|^2 - |\beta|^2)^2} \\ &= \underbrace{\frac{1+\epsilon^2}{(1-\epsilon^2)^2}}_{\text{Impact of gain imb.}} \times \underbrace{\frac{1}{\cos^2(\phi)}}_{\text{Impact of phase imb.}} . \end{aligned} \tag{34}$$

In summary, **in SCM systems the quadrature error of the modulator (Tx) cannot be perfectly compensated at the receiver side and a degradation of the signal-to-noise ratio (SNR) of** $\gtrsim 10\log_{10}(F)[dB]$ **will be experienced**[2]. It is interesting to realize that this conclusion does not agree with that reported in [2], where it has been found that the transmitter I/Q imbalance can be compensated without any performance degradation. This discrepancy is caused due to the model used in [2] to add I/Q imbalance as a result of experimental setup limitations (i.e., the I/Q imbalance is added at the receiver side; see pag. 2, second column, last paragraph).

B. Case 2: Impact of I/Q Skew ($\epsilon = 0$ and $\phi = 0$)

In this case, we get

$$\begin{aligned} f(t) &= \frac{1}{2}\left[\delta(t+\tau/2) + \delta(t-\tau/2)\right], \\ \overline{f}(t) &= \frac{1}{2}\left[\delta(t+\tau/2) - \delta(t-\tau/2)\right], \end{aligned}$$

[1]It is possible to show that $|\alpha|^2 + |\beta|^2 = 1 + \epsilon^2$ while $|\alpha|^2 - |\beta|^2 = (1-\epsilon^2)\cos(\phi)$.

[2]A linear transformation at the Tx should be considered to mitigate this *fundamental* degradation experienced at the Rx.

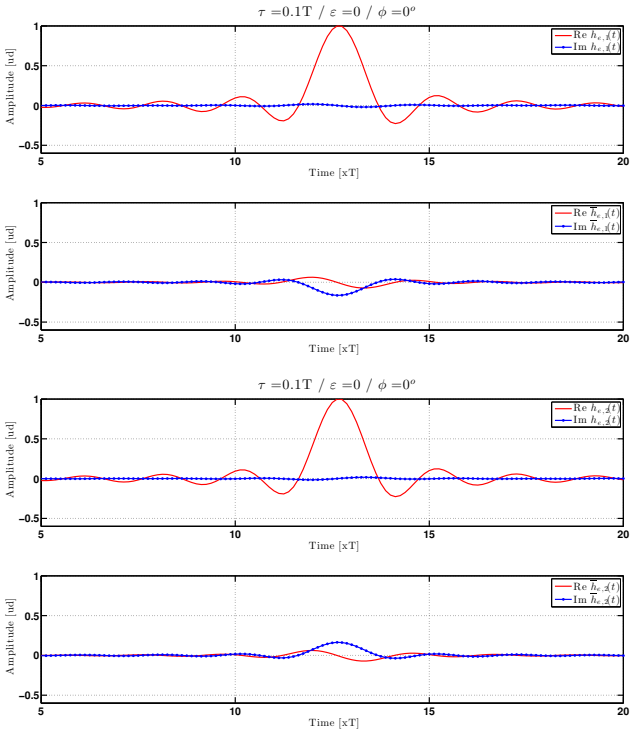

Figure 2. Example of the channel responses for $\tau = 0.1T$, $\epsilon = 0$, and $\phi = 0$.

thus, and taking into account that $g(t)$ is a real pulse, we obtain

$$h_{e,1}(t) = \frac{1}{2}\left[e^{j\omega_c\tau/2}g(t+\tau/2) + e^{-j\omega_c\tau/2}g(t-\tau/2)\right],$$
$$h_{e,2}(t) = \frac{1}{2}\left[e^{-j\omega_c\tau/2}g(t+\tau/2) + e^{j\omega_c\tau/2}g(t-\tau/2)\right] = h_{e,1}^*(t),$$
$$\overline{h}_{e,1}(t) = \frac{1}{2}\left[e^{-j\omega_c\tau/2}g(t+\tau/2) - e^{j\omega_c\tau/2}g(t-\tau/2)\right],$$
$$\overline{h}_{e,2}(t) = \frac{1}{2}\left[e^{j\omega_c\tau/2}g(t+\tau/2) - e^{-j\omega_c\tau/2}g(t-\tau/2)\right] = \overline{h}_{e,1}^*(t).$$

When τ is small (e.g.,$|\tau| < 0.2T$), we can get

$$h_{e,1}(t) = h_{e,2}(t) \approx \cos(\omega_c\tau/2)g(t), \tag{35}$$
$$\overline{h}_{e,1}(t) = \overline{h}_{e,2}^*(t) \approx -j\sin(\omega_c\tau/2)g(t). \tag{36}$$

Figure 2 depicts an example of the equivalent baseband channel responses for $\tau = 0.1T$, $\epsilon = 0$, and $\phi = 0$ derived from simulations. Again, we can confirm the results predicted from the theory.

In order to provide a simple approach to know the impact of the Tx I/Q skew on the receiver performance, we consider the same example used previously in Section II-A based on (35) and (36). Thus, it is possible to show that

$$\begin{bmatrix} r_{1,x}(n) \\ r_{2,x}^*(n) \end{bmatrix} = \mathbf{M}_\tau \begin{bmatrix} a_{1,n} \\ a_{2,n}^* \end{bmatrix} \tag{37}$$

where

$$\mathbf{M}_\tau = \begin{bmatrix} \cos(\omega_c\tau/2) & j\sin(\omega_c\tau/2) \\ j\sin(\omega_c\tau/2) & \cos(\omega_c\tau/2) \end{bmatrix}. \tag{38}$$

Notice that $\mathbf{M}_\tau$ is an unitary matrix with determinant unitary, therefore *the effect of the I/Q skew could be perfectly compensated at the receiver*. We highlight that this result has been derived from (35) and (36), which assume that the ISI of the channel pulses is negligible. As we shall show later, the accuracy of this approach is satisfactory for QPSK, however it degrades for QAM16.

C. Case 3: Impact of I/Q Skew and Quadrature Error

Similarly, it is possible to show that

$$\begin{aligned}
h_{e,1}(t) &= \frac{(\alpha+\beta)}{2}e^{j\omega_c\tau/2}g(t+\tau/2) + \frac{(\alpha-\beta)}{2}e^{-j\omega_c\tau/2}g(t-\tau/2), \\
h_{e,2}(t) &= \frac{(\alpha+\beta)}{2}e^{-j\omega_c\tau/2}g(t+\tau/2) + \frac{(\alpha-\beta)}{2}e^{j\omega_c\tau/2}g(t-\tau/2), \\
\overline{h}_{e,1}(t) &= \frac{(\alpha+\beta)}{2}e^{-j\omega_c\tau/2}g(t+\tau/2) - \frac{(\alpha-\beta)}{2}e^{j\omega_c\tau/2}g(t-\tau/2), \\
\overline{h}_{e,2}(t) &= \frac{(\alpha+\beta)}{2}e^{j\omega_c\tau/2}g(t+\tau/2) - \frac{(\alpha-\beta)}{2}e^{-j\omega_c\tau/2}g(t-\tau/2).
\end{aligned}$$

Since α and β are complex numbers in general, note that $|h_{e,1}(t)| \neq |h_{e,2}(t)|$ and $|\overline{h}_{e,1}(t)| \neq |\overline{h}_{e,2}(t)|$. Figure 3 depicts an example of the equivalent baseband channel responses for $\tau = 0.2T$, $\epsilon = 0.2$, and $\phi = 20^o$ derived from simulation. Unlike the previous examples, we see important differences between the magnitudes of the responses $\overline{h}_{e,1}(t)$ and $\overline{h}_{e,2}(t)$. This shows that the impact of the combined effects on the performance should be different in both channels.

When τ is small (e.g.,$|\tau| < 0.2T$), it is possible to show that

$$\begin{bmatrix} r_{1,x}(n) \\ r_{2,x}^*(n) \end{bmatrix} = \mathbf{M}_{\phi,\epsilon}\mathbf{M}_\tau \begin{bmatrix} a_{1,n} \\ a_{2,n}^* \end{bmatrix} \tag{39}$$

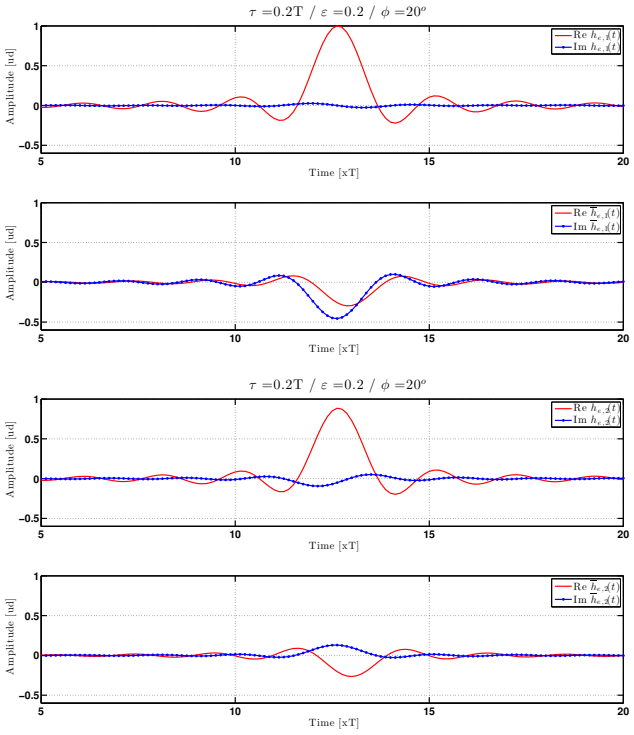

Figure 3. Example of the channel responses for $\tau = 0.2T$, $\epsilon = 0.2$, and $\phi = 20^o$

where $\mathbf{M}_{\phi,\epsilon}$ and $\mathbf{M}_{\tau}$ are given by (32) and (38), respectively. Therefore previous observations are still valid in the presence of the combined effects of I/Q skew and quadrature errors (e.g., the I/Q skew could be perfectly compensated at the receiver).

III. Reduced Complexity I/Q Skew Compensator

In order to compensate the effects of the I/Q skew and quadrature error introduced on the transmitter side on SCM schemes, an 8×8 MIMO equalizer operating at symbol rate can be implemented [1]. Such an equalizer is supposed to be used after the PMD equalization, carrier recovery, cycle slips correction and timing synchronization are achieved on the DSP. In this initial approach, the equalizer must have 8×8 = 64 filters of N taps in time domain. This operation

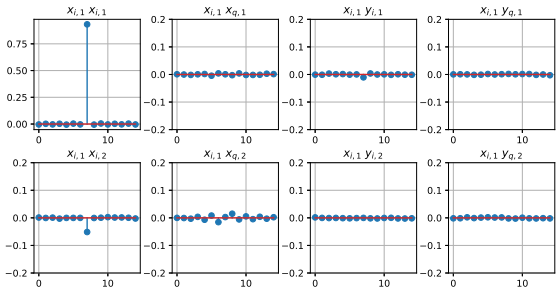

Figure 4. Example of the equalizer taps.

can be expressed as

$$\begin{bmatrix} s_{x_i,1} \\ s_{x_q,1} \\ s_{y_i,1} \\ s_{y_q,1} \\ s_{x_i,2} \\ s_{x_q,2} \\ s_{y_i,2} \\ s_{y_q,2} \end{bmatrix} = \begin{bmatrix} f_{11} & f_{12} & f_{13} & f_{14} & f_{15} & f_{16} & f_{17} & f_{18} \\ f_{21} & f_{22} & f_{23} & f_{24} & f_{25} & f_{26} & f_{27} & f_{28} \\ f_{31} & f_{32} & f_{33} & f_{34} & f_{35} & f_{36} & f_{37} & f_{38} \\ f_{41} & f_{42} & f_{43} & f_{44} & f_{45} & f_{46} & f_{47} & f_{48} \\ f_{51} & f_{52} & f_{53} & f_{54} & f_{55} & f_{56} & f_{57} & f_{58} \\ f_{61} & f_{62} & f_{63} & f_{64} & f_{65} & f_{66} & f_{67} & f_{68} \\ f_{71} & f_{72} & f_{73} & f_{74} & f_{75} & f_{76} & f_{77} & f_{78} \\ f_{81} & f_{82} & f_{83} & f_{84} & f_{85} & f_{86} & f_{87} & f_{88} \end{bmatrix} \otimes \begin{bmatrix} r_{x_i,1} \\ r_{x_q,1} \\ r_{y_i,1} \\ r_{y_q,1} \\ r_{x_i,2} \\ r_{x_q,2} \\ r_{y_i,2} \\ r_{y_q,2} \end{bmatrix}, \tag{40}$$

where $\otimes$ denotes sum of convolution and f_{ij} is the impulse response of the equalizer corresponding to the i-th output due to j-th input.

As explained in previous sections, the output for each lane is observed to be dependent on the input for the same lane and the inputs for the lanes on the other sub channel corresponding to the same polarization. This means that the output for each lane depends only on 3 lane inputs, i.e. a total of 3 $\times$ 8 = 24 filters of N taps, which reduces significantly the complexity comparing with the initial proposal of 64 filters of the same length. Next figure shows the filter responses with $N = 15$ for QAM16 with 1 ps of I/Q skew at an aggregate symbol rate of 66 GBd (2 $\times$ 33 GBd). For example, we see that only lanes $x_{i,2}$ and $x_{q,2}$ of the Channel 2 contribute to the output $x_{i,1}$ of the Channel 1. Moreover, the filter responses on the principal diagonal are impulses, i.e., only a delay line. Thus, the I/Q compensator reduces to

$$\begin{bmatrix} s_{x_i,1} \\ s_{x_q,1} \\ s_{y_i,1} \\ s_{y_q,1} \\ s_{x_i,2} \\ s_{x_q,2} \\ s_{y_i,2} \\ s_{y_q,2} \end{bmatrix} \approx \begin{bmatrix} \delta & 0 & 0 & 0 & f_{15} & f_{16} & 0 & 0 \\ 0 & \delta & 0 & 0 & f_{25} & f_{26} & 0 & 0 \\ 0 & 0 & \delta & 0 & 0 & 0 & f_{37} & f_{38} \\ 0 & 0 & 0 & \delta & 0 & 0 & f_{47} & f_{48} \\ f_{51} & f_{52} & 0 & 0 & \delta & 0 & 0 & 0 \\ f_{61} & f_{62} & 0 & 0 & 0 & \delta & 0 & 0 \\ 0 & 0 & f_{73} & f_{74} & 0 & 0 & \delta & 0 \\ 0 & 0 & f_{83} & f_{84} & 0 & 0 & 0 & \delta \end{bmatrix} \otimes \begin{bmatrix} r_{x_i,1} \\ r_{x_q,1} \\ r_{y_i,1} \\ r_{y_q,1} \\ r_{x_i,2} \\ r_{x_q,2} \\ r_{y_i,2} \\ r_{y_q,2} \end{bmatrix}, \tag{41}$$

where δ denotes the (delayed) impulse function.

The previous simplifications assume that:

- Carrier and phase recovery are achieved previously.
- The PMD equalizers of both sub-channels have converged on the correct polarizations and without skew between them. For example, if the polarization X was exchanged with Y on one of the sub channels, the output lane of the polarization for one sub channel would depend on the opposite polarization of the opposite sub channel, and the filters on the opposite sub-channel but same polarization will have null coefficients. On the other hand, the (symbol) skew between sub-channels may require filters with more taps. These effects (i.e., proper convergence and skew of the sub-channels) can be detected by the Framer block.
- There were no cycle slips (CS) on both sub channels. Similarly to the *synchronous equalizer*, CS correction is required before the MIMO equalizer.

IV. Numerical Results

The I/Q compensator was implemented and simulated on a floating-point simulator, implementing both the full filters mode (40) and the simplified mode (41). Next figures show the penalty vs the I/Q skew introduced on the transmitter side. The channel is a non-dispersive optical channel with ASE noise and a frequency rotation of the state of polarizations of 5 kHz. Also, the receiver laser has a frequency offset of 200 MHz with respect to transmitter laser. The MIMO equalizer convergence starts once all the other DSP modules have converged. We use N =21 taps on each filter of the MIMO equalizer.

We compare the performance of both uncompensated and compensated receivers (full and simplified compensator are included). Firstly, only TX I/Q skew is introduced, and then we add

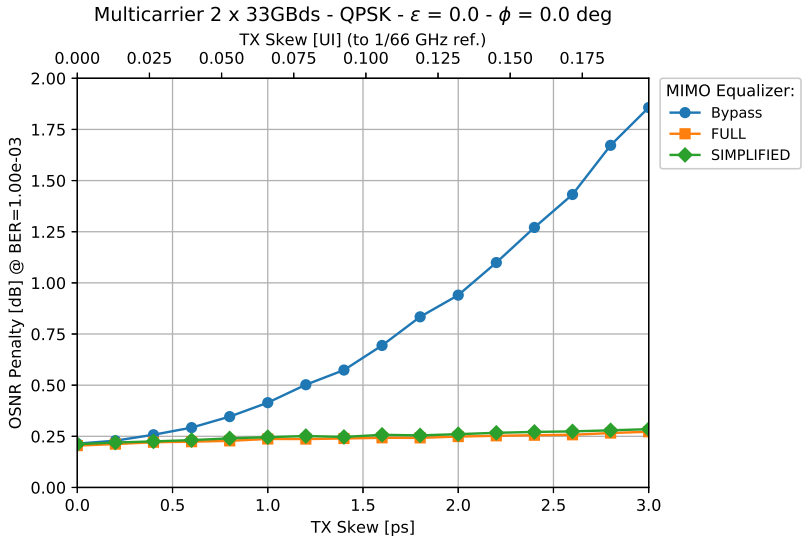

Figure 5. Simulation results for QPSK with $\epsilon = 0$ and $\phi = 0$.

quadrature error with amplitude imbalance of $\epsilon = 0.1$ and phase errors $\phi = \pm 15^o$. Notice that in the absence of I/Q skew ($\tau = 0$), SNR penalty after the optimal compensator for $\epsilon = 0.1$ and $|\phi| = 15^o$ will be (at least)

$$10\log_{10}(F) = 10\log_{10}\left[\frac{1+\epsilon^2}{(1-\epsilon^2)^2\cos^2(\phi)}\right] = 0.43dB.$$

QPSK and QAM16 are simulated with two subcarrier channels of 33 GBd, making an aggregate symbol rate of 66 GBd. It can be seen that QAM16 is less robust than QPSK. In QAM16, notice that the DSP cannot converge without the compensator of I/Q skew and quadrature errors. In all the cases, we verify that **the performance of the proposed reduced complexity compensator is similar to the one achieved by the *full* solution proposed in [1]**.

Figs. 11 and 12 show the SNR penalty versus phase and gain imbalances with $\tau = 0$. For QPSK we observe that simulations agrees very well with the theoretical values derived from (34). The accuracy of (34) degrades with QAM16 as a result of the impact of the quadrature errors on the other DSP algorithms (e.g., carrier recovery, PMD equalizer, etc.). Finally, Figs. 13 and 14 show a comparative of the performance by using a different number of taps on the equalizers. We can infer that $N = 7$ taps seems to be satisfactory for the cases considered in this report. Therefore, the proposed reduced complexity I/Q compensation approach could be considered for implementing with *low* impact on the power consumption.

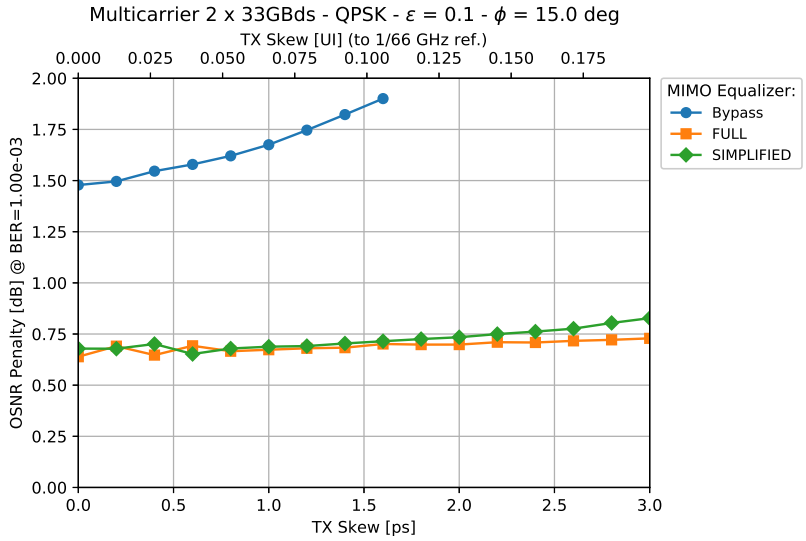

Figure 6. Simulation results for QPSK with $\epsilon = 0.1$ and $\phi = 15^o$.

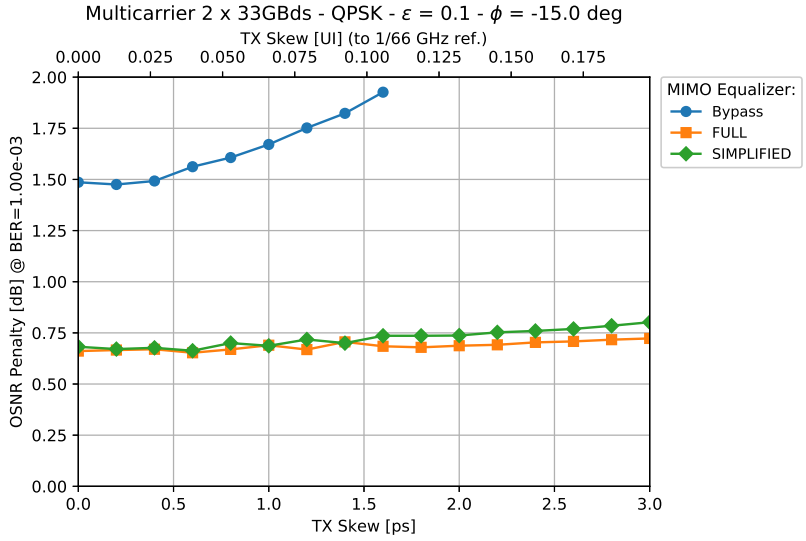

Figure 7. Simulation resultsfor QPSK with $\epsilon = 0.1$ and $\phi = -15^o$.

REFERENCES

[1] G. Bosco et al., "Impact of the transmitter IQ-skew in multi-carrier coherent optical systems," *OFC*, 2016.

[2] E. Porto da Silva and D. Zibar, "Widely linear equalization for IQ imbalance and skew compensation in multicarrier systems," *ECOC*, September 2016.

[3] E. Porto da Silva and D. Zibar, "Widely linear equalization for IQ imbalance and skew compensation in optical coherent receivers," *J. Lightwave Technol.*, March 2016.

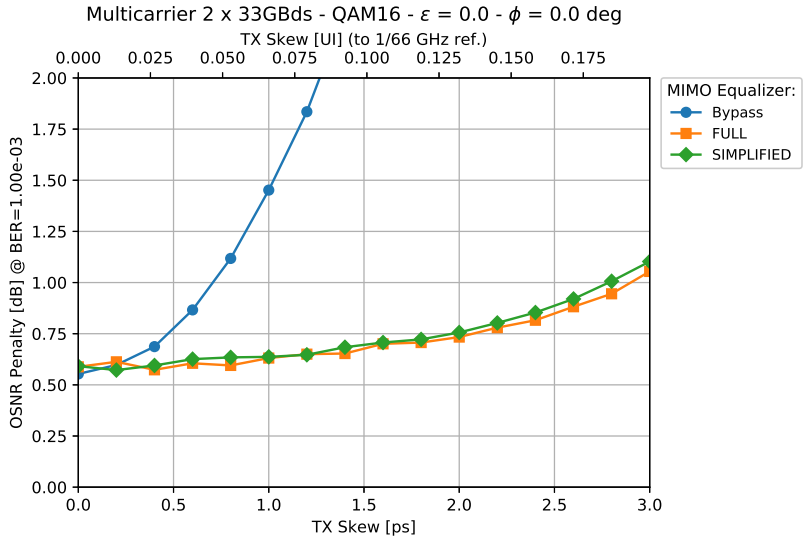

Figure 8. Simulation results for QAM16 with $\epsilon = 0$ and $\phi = 0^o$.

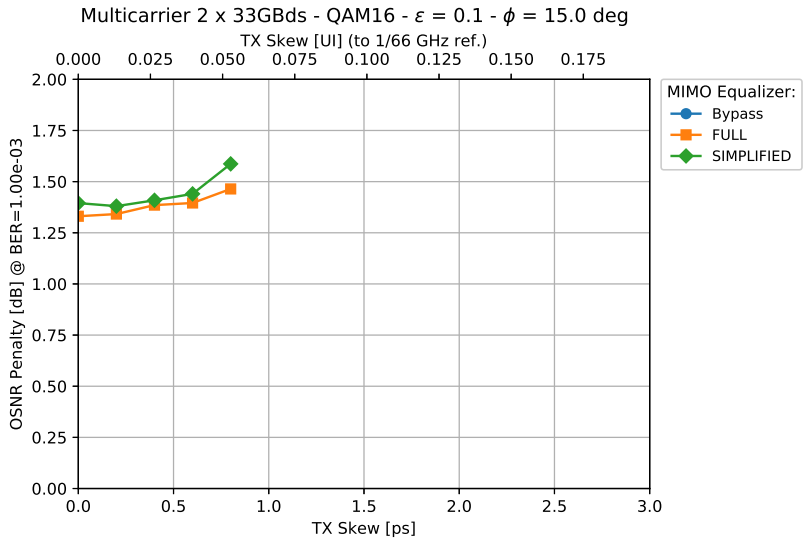

Figure 9. Simulation results for QAM16 with $\epsilon = 0.1$ and $\phi = 15^o$.

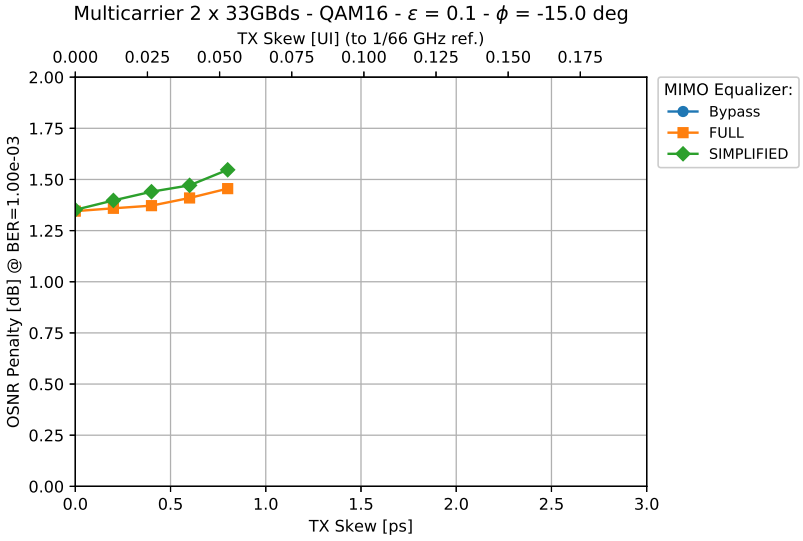

Figure 10. Simulation results for QAM16 with $\epsilon = 0.1$ and $\phi = -15^o$.

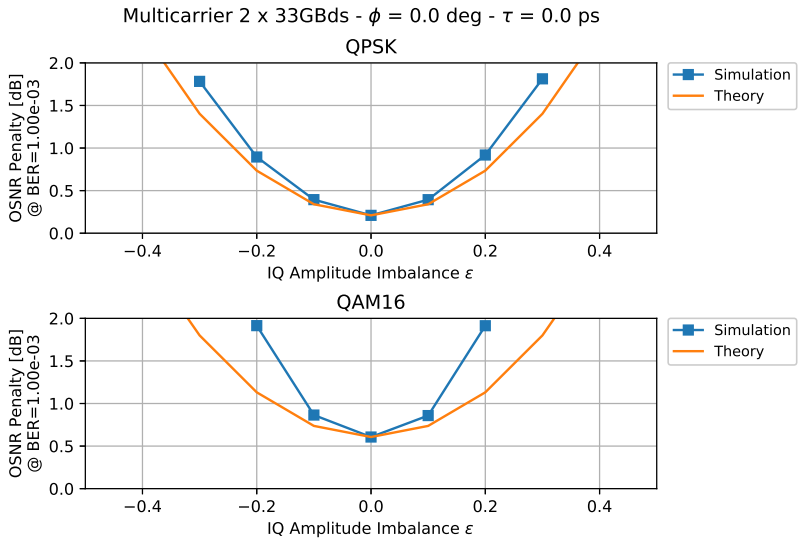

Figure 11. SNR penalty versus the amplitude error ϵ.

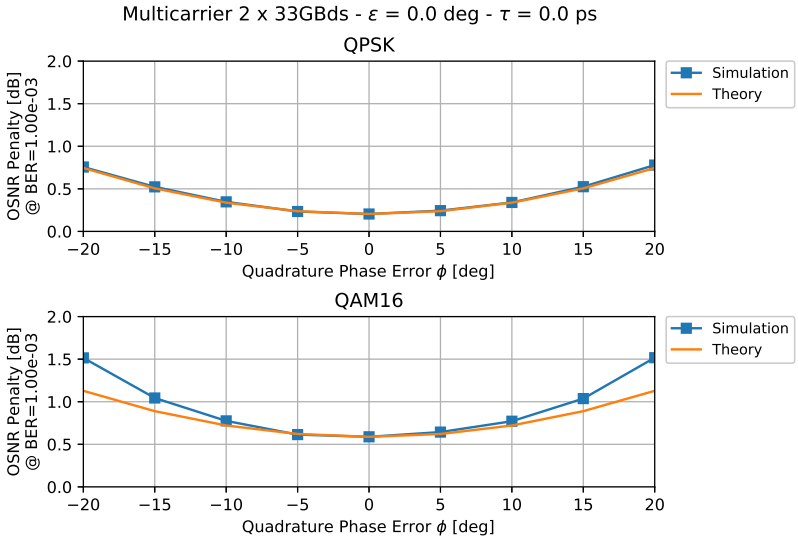

Figure 12. SNR penalty versus the phase error ϕ.

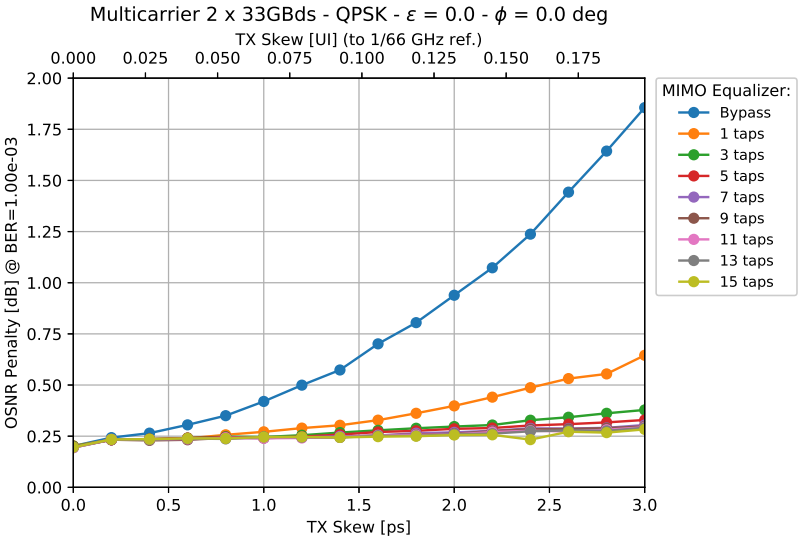

Figure 13. Impact of the number of taps.

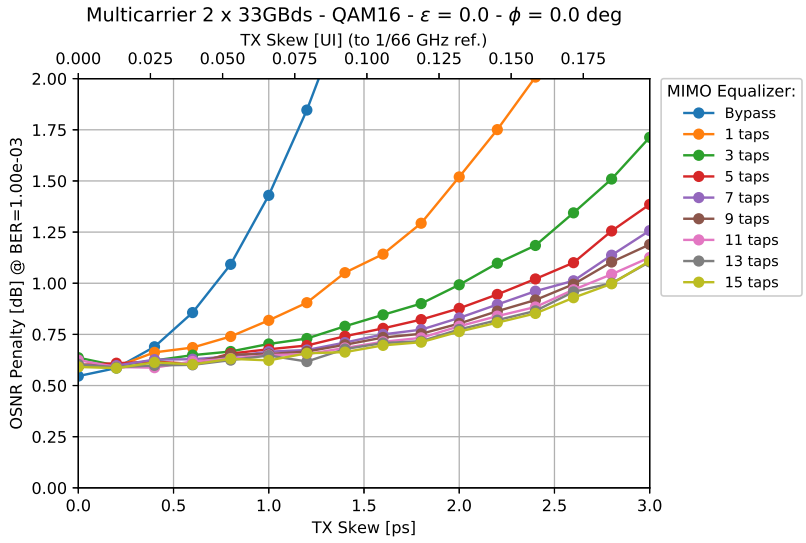

Figure 14. Impact of the number of taps.